Published in final edited form as:
Free Radic Biol Med. 2012 March 15; 52(6): 1075–1085. doi:10.1016/j.freeradbiomed.2011.12.024.

Inactivation of thiol-dependent enzymes by hypothiocyanous acid: role of sulfenyl thiocyanate and sulfenic acid intermediates

Tessa J. Barrett[a,b], **David I. Pattison**[a,b], **Stephen E. Leonard**[c,1], **Kate S. Carroll**[d], **Michael J. Davies**[a,b], and **Clare L. Hawkins**[a,b,*]

[a]The Heart Research Institute, Newtown, NSW 2042, Australia

[b]Sydney Medical School, University of Sydney, Sydney, NSW 2006, Australia

[c]Chemical Biology Graduate Program, University of Michigan, Ann Arbor, MI 48109, USA

[d]Department of Chemistry, The Scripps Research Institute, Jupiter, FL 33458, USA

Abstract

Myeloperoxidase (MPO) forms reactive oxidants including hypochlorous and hypothiocyanous acids (HOCl and HOSCN) under inflammatory conditions. HOCl causes extensive tissue damage and plays a role in the progression of many inflammatory-based diseases. Although HOSCN is a major MPO oxidant, particularly in smokers, who have elevated plasma thiocyanate, the role of this oxidant in disease is poorly characterized. HOSCN induces cellular damage by targeting thiols. However, the specific targets and mechanisms involved in this process are not well defined. We show that exposure of macrophages to HOSCN results in the inactivation of intracellular enzymes, including creatine kinase (CK) and glyceraldehyde-3-phosphate dehydrogenase (GAPDH). In each case, the active-site thiol residue is particularly sensitive to oxidation, with evidence for reversible inactivation and the formation of sulfenyl thiocyanate and sulfenic acid intermediates, on treatment with HOSCN (less than fivefold molar excess). Experiments with DAz-2, a cell-permeable chemical trap for sulfenic acids, demonstrate that these intermediates are formed on many cellular proteins, including GAPDH and CK, in macrophages exposed to HOSCN. This is the first direct evidence for the formation of protein sulfenic acids in HOSCN-treated cells and highlights the potential of this oxidant to perturb redox signaling processes.

Keywords

Myeloperoxidase; Hypothiocyanous acid; Sulfenic acid; Protein oxidation; Macrophage; Free radicals

Myeloperoxidase (MPO)[2] catalyzes the reaction of hydrogen peroxide (H_2O_2) with halide and pseudohalide ions (Cl^-, Br^-, I^-, and thiocyanate, SCN^-) to form hypohalous acids (hypochlorous acid, HOCl, from Cl^-; hypobromous acid, HOBr, from Br^-; and hypothiocyanous acid, HOSCN, from SCN^-), which are potent oxidants (reviewed in [1,2]). SCN^- is the favored substrate of MPO and many other peroxidase enzymes (inclusive of eosinophil peroxidase and lactoperoxidase), which results in the formation of HOSCN in a

*Corresponding author at: The Heart Research Institute, Newtown, NSW 2042, Australia. Fax: +61 2 9565 5584. hawkinsc@hri.org.au (C.L. Hawkins).
[1]Current address: Department of Chemistry, University of Washington, Seattle, WA 98195-1700, USA.

Appendix A. Supplementary data

Supplementary data to this article can be found online at doi:10.1016/j.freeradbiomed.2011.12.024.

variety of physiological settings [3–7]. It is postulated that HOSCN production is particularly important in smokers, owing to the higher levels of SCN^- in their plasma from detoxification of cyanide in cigarette smoke [8]. The hypohalous acids are powerful antibacterial agents and, as such, play an important role in the human immune system [9]. However, recent evidence suggests that these oxidants can also induce host cell damage, particularly under inflammatory conditions, which may contribute to the development of a number of diseases, including atherosclerosis, neurodegenerative disorders, arthritis, and some cancers (reviewed in [1,2]).

HOCl and HOBr have been implicated in a number of pathologies owing to the detection of elevated levels of their biomarkers 3-chloro-Tyr and 3-bromo-Tyr, respectively, in diseased tissues and inflammatory fluids [2,10–12]. In contrast, the role of HOSCN in disease has not been widely studied [13]. Serum SCN^- levels correlate with the extent of fatty streak formation and macrophage foam cell populations, consistent with a role for HOSCN in atherosclerosis [14,15]. Moreover, cyanate (OCN^-) formation from the decomposition of HOSCN has been implicated as the major pathway for inducing elevated homocitrulline formation in atherosclerosis in humans [16]. However, HOSCN production has also been proposed to be beneficial, by preventing disease through the detoxification of other, more potent, oxidants such as HOCl (e.g., [17,18]). Similarly, there is some controversy regarding the role of HOSCN in the induction of mammalian cell damage [19,20].

It is well established that exposure of bacteria, mammalian cells, and plasma to HOSCN results in specific and selective damage to thiols (reviewed in [13,21]). This targeting of thiols results in the inhibition of bacterial glycolysis via inactivation of the glycolytic enzymes glyceraldehyde-3-phosphate dehydrogenase (GAPDH), hexokinase, glucose-6-phosphate dehydrogenase, and aldolase [22–24]. Similarly, HOSCN depletes thiols and inactivates thiol-dependent enzymes, including GAPDH, caspases, glutathione transferases, membrane ATPases, and protein tyrosine phosphatases in mammalian cells [5,20,25]. HOSCN can also perturb various cell signaling pathways, with evidence for alterations in the phosphorylation of mitogen-activated protein kinase proteins and the release of inflammatory mediators in macrophages and endothelial cells [25–27]. In macrophages, HOSCN is a potent inducer of cellular apoptosis [20], though in human umbilical vein endothelial cells, this oxidant induces cell damage via alternative pathways [19]. In each case, these cellular effects are attributed to the selectivity of HOSCN for thiol-containing proteins [19,20,25–27].

Reaction of HOSCN with thiols results in the generation of sulfenyl thiocyanate derivatives (RS–SCN; Reaction (1)), which are postulated to hydrolyze to sulfenic acid intermediates (RS–OH; Reaction (2)) [22,28]:

$$RS-H+HOSCN \rightarrow RS-SCN \quad (1)$$

$$RS-SCN+H_2O \rightarrow RS-OH+SCN^-+H^+ \quad (2)$$

Sulfenyl species have been reported in bacterial cells exposed to HOSCN, though direct evidence for protein sulfenic acid formation is lacking, owing to a lack of specificity in the methods used to assess these reactive species [22,29]. Similarly, although there are data on the targets of HOSCN in mammalian cells [5,20,25] there is little information available regarding the nature of the intermediates and mechanisms involved in thiol-dependent enzyme inactivation.

In this study, we examine the mechanism involved in HOSCN-mediated inactivation of GAPDH and creatine kinase (CK), both in isolation and in the cellular environment. We show that HOSCN induces enzyme inactivation in both a reversible and a nonreversible manner via the formation of sulfenyl thiocyanate/sulfenic acid intermediates and sulfinic/sulfonic acids, respectively. In addition, we provide the first direct experimental evidence for the formation of protein sulfenic acid intermediates in mammalian cells exposed to HOSCN. This suggests that HOSCN may have the potential to act as a second messenger in redox signaling processes, which has important implications for the development of inflammatory disease.

Materials and methods

Reagents

Aqueous solutions and buffers were prepared using Nanopure water filtered through a four-stage Milli-Q system (Millipore–Waters, Lane Cove, NSW, Australia). All proteins and 5-thio-2-nitrobenzoic acid (TNB) solutions were prepared in 0.1 M sodium phosphate buffer (pH 7.4) pretreated with Chelex resin (Bio-Rad, Hercules, CA, USA) to remove contaminating trace metal ions. Dimedone (505 mM; Sigma–Aldrich, Castle Hill, NSW, Australia) was prepared in 95% (v/v) ethanol. Lactoperoxidase (LPO; from bovine milk; Merck, Whitehouse Station, NJ, USA) was quantified by absorbance at 412 nm using ε 112,000 M^{-1} cm^{-1} [30]. H_2O_2 (30% v/v solution; Merck) was quantified at 240 nm using ε 39.4 M^{-1} cm^{-1} [31]. CK (from rabbit muscle) was obtained from Roche (Castle Hill, NSW, Australia), and GAPDH (from rabbit muscle) from Sigma–Aldrich.

Cell culture

Murine macrophage-like J774A.1 cells (American Type Culture Collection; No. 915051511) were cultured under sterile conditions in Dulbecco's modified Eagle's medium (Sigma–Aldrich) supplemented with 10% (v/v) fetal bovine serum (Sigma–Aldrich) and 2 mM L-glutamine (Thermotrace, Melbourne, VIC, Australia). Cells were seeded at 1×10^6 cells ml^{-1} in 12-well plates and allowed to adhere overnight. Before treatment, the medium was removed and cells were washed twice with phosphate-buffered saline (PBS; Amresco, Solon, OH, USA). Cells were washed twice with PBS after treatment and before lysis in 600 μl of H_2O and centrifugation at 8000 *g* at 4 °C for 5 min. Protein concentrations were determined using the bicinchoninic acid assay (Pierce, Rockford, IL, USA) using bovine serum albumin (BSA) standards (Sigma–Aldrich).

Generation and quantification of HOSCN

HOSCN was produced enzymatically from the reaction of H_2O_2 with SCN^- in the presence of LPO as described previously [20,32]. The concentration of HOSCN was quantified immediately using the TNB assay [20,32,33] with absorbances recorded at 412 nm and ε 14,150 M^{-1} cm^{-1} [34]. Stock solutions of HOSCN were diluted into potassium phosphate buffer (10 mM, pH 6.6) for protein and cell lysate experiments or PBS for intact cell experiments.

$S^{14}CN^-$ incorporation studies with $HOS^{14}CN$

$HOS^{14}CN$ was prepared as above except using $KS^{14}CN$ (3.75 mM) (American Radiolabeled Chemicals, St. Louis, MO, USA) and 1.875 mM H_2O_2, as previously described [32]. $HOS^{14}CN$ was added to CK or GAPDH (25 μM) and incubated for 5 or 30 min, respectively, before precipitation with 10% (w/v) trichloroacetic acid (TCA). Proteins were pelleted by centrifugation (10,000 *g* for 5 min at 4 °C), and free $S^{14}CN^-$ label was removed by washing pellets twice with 5% (w/v) TCA and twice with ice-cold acetone. Protein

pellets were air-dried and resuspended in 100 μl of formic acid before addition to 5 ml of Ultima Gold scintillant (PerkinElmer, Waltham, MA, USA) and liquid scintillation counting on a Packard Tri-Carb liquid scintillation counter (2100TR; PerkinElmer). To assess whether $S^{14}CN^-$ incorporation was reversible, dithiothreitol (DTT; 1.25 mM) or H_2O was added 15 min post-HOS^{14}CN incubation before precipitation with TCA. Control experiments to assess nonspecific binding of $S^{14}CN^-$ to the protein were performed using solutions prepared in the absence of LPO in each case.

Dimedone specificity studies with $S^{14}CN^-$ incorporation

Equimolar HOS^{14}CN was added to GAPDH (25 μM) for 30 min before further incubation in the presence of dimedone (5 mM) or ethanol as control for 2 h at 22 °C. Protein was precipitated and washed and ^{14}C incorporation assessed as described above.

Quantification of protein thiols

The extent of protein thiol oxidation was assessed using the thiol-specific reagent ThioGlo-1 (Merck) as described previously [25,33]. Thiol concentrations were quantified by fluorescence spectroscopy at λ_{ex} 360 nm and λ_{em} 530 nm using glutathione (GSH; Sigma–Aldrich) to construct a standard curve.

Enzyme activity assays

GAPDH activity was measured by monitoring the formation of NADH after addition of glyceraldehyde 3-phosphate (GAP) [35]. Cell lysate (20 μl) was combined with 120 μl of phosphate buffer (28.5 mM sodium pyrophosphate, 38 mM sodium phosphate buffer, pH 7.4) and 60 μl of NAD^+/GAP substrate solution (1.2 mM GAP, 2.5 mM NAD^+) on a 96-well plate. The plate was shaken briefly and GAPDH activity measured as the rate of absorbance increase at 340 nm over 10 min (20 s cycles) at 37 °C, on a Flexstation 3 plate reader (Molecular Devices, Sunnyvale, CA, USA).

CK activity was determined using a thymol blue-based assay. Cell lysate (100 μl) was combined with 100 μl of 5 mM borate buffer containing 5 mM magnesium acetate, 0.01% (w/v) thymol blue, 24 mM creatine, and 4 mM ATP, on a 96-well plate in triplicates. Enzyme activity was measured as the rate of absorbance loss at 597 nm over a 10 min interval (30 s cycles) at 22 °C, on a Benchmark Plus plate reader (Bio-Rad).

Derivatization of protein sulfenic acids with dimedone

CK and GAPDH (25 μM) were treated with HOSCN (12.5–125 μM) for 5 and 30 min, respectively. Dimedone (5 mM) was added, and after 2 h agitation at 22 °C, proteins were precipitated by the addition of 5% (w/v) TCA and pelleted by centrifugation (7500 *g* for 5 min at 4 °C). Pellets were solubilized, reduced, and alkylated as described previously [32]. Proteins were digested by the addition of sequencing-grade trypsin (Promega, Madison, WI, USA) at protein: trypsin ratios (w/w) of 210:1 and 180:1 for CK and GAPDH, respectively, with overnight incubation at 37 °C. Digestion was terminated by acidification with trifluoroacetic acid (TFA; 0.02% v/v).

LC–MS peptide mass mapping studies

Peptide LC–MS analyses were performed in the positive-ion mode with a Thermo Finnigan LCQ Deca XP Max ion trap mass spectrometer coupled to a Thermo Finnigan Surveyor HPLC system (Thermo Electron Corp., Rydalmere, NSW, Australia). Tryptic peptides were separated on a reverse-phase C-18 column (Zorbax ODS 5 μm; 3.0 × 250 mm; Agilent Technologies, Forest Hill, VIC, Australia) at 30 °C, at a flow rate of 0.4 ml min^{-1}. The mobile phases employed were 0.1% (v/v) TFA in water as solvent A and 0.1% (v/v) TFA in

acetonitrile as solvent B. Peptides were eluted using the following gradient: 10–30% B over 15 min, 30–80% B over 20 min, then a wash phase of 100% B for 5 min before an equilibration step of 10% B for 10 min. The electrospray needle was held at 4500 V. Nitrogen, the sheath gas, was held at 80 units. The collision gas was helium. The temperature of the heated capillary was 250 °C. For MS/MS studies the normalized collision energy was set at 35%.

Derivatization of cellular proteins with DAz-2 and preparation of lysates

J774A.1 cells were seeded at 1×10^6 cells ml^{-1} in 12-well plates and allowed to adhere overnight. Cells were washed twice with PBS, before incubation with DAz-2 (5 mM) or dimethyl sulfoxide (DMSO; 1% v/v) for control experiments at 37 °C for 30 min, with gentle mixing. In the presence of DAz-2 or DMSO, cells were treated with PBS or HOSCN (50 and 100 μM) for an additional 15 min at 37 °C. After oxidant exposure, cells were washed with PBS, lysed in cold lysis buffer (50 mM Tris, pH 8.0, 150 mM NaCl, 1% NP-40, 2× protease inhibitor (Roche)), and incubated on ice for 20 min. Lysates were centrifuged at 4 °C for 20 min, at 10,000 *g*, and supernatant was collected. Staudinger ligation to biotinylated DAz-2-labeled proteins was performed by the incubation of the lysates (approx 190 μg protein) with p-biotin (200 μM) and DTT (5 mM) for 2 h at 37 °C. Reaction was quenched by the addition of 1 ml ice-cold acetone and incubation at −80 °C for 2 h or overnight. Protein pellets were collected by centrifugation (4 °C, 20 min, 10,000 *g*) before being washed with 200 μl acetone, suspended in LDS sample buffer (Invitrogen, Carlsbad, CA, USA), and heated at 70 °C for 10 min.

Western blot and protein staining

Cellular proteins were separated by SDS–PAGE on a NuPAGE Novex 4–12% Bis–Tris minigel (Invitrogen) and transferred to a polyvinylidene difluoride (PVDF) membrane (Invitrogen) using an iBlot transfer system (Invitrogen). Membranes were blocked in 5% BSA in PBS–Tween 20, incubated with 1:10,000 horseradish peroxidase (HRP)–streptavidin (Thermo Fisher, Waltham, MA, USA), and developed with ECL Plus chemiluminescence reagents (GE Healthcare, Waukesha, WI, USA). Signals were directly digitized using a ChemiDoc XRS (Bio-Rad). To assess the location of GAPDH on the membrane, membranes were stripped and probed with anti-GAPDH (Abcam) and donkey anti-mouse–HRP as the secondary antibody (GE Healthcare). Protein identification was determined by gel band excision, tryptic digestion, and LC–MS/MS (QSTAR Elite). To verify equal protein loading, membranes were stained with 0.05% Coomassie R-250 (Sigma–Aldrich) in isopropanol/acetic acid/water (50/20/30) for 2 h, destained for 1 h with isopropanol/acetic acid/H_2O (12.5/10/77.5), washed with water. and allowed to air-dry.

In-gel digestion and protein identification by LC–MS/MS

Protein bands of interest were excised from gels, by overlaying Coomassie-stained gels on Coomassie-stained PVDF membranes, to confirm the location of bands predicted to contain CK or GAPDH. Gel bands were then washed, proteins were digested, and sample cleanup was performed as previously described [36]. Mass spectrometric analysis was performed on a Q-TOF hybrid quadrupole/orthogonal-acceleration time-of-flight mass spectrometer as described previously [37]. Analysis was performed by the proteomics facility at the University of Sydney. MS/MS data analysis was undertaken utilizing Mascot (Matrix Science) software. ESI-QUAD-TOF data were searched in the Swiss-Prot database, utilizing the *Mus musculus* (house mouse) proteome. Mascot was searched with a fragment ion mass tolerance of 0.50 Da and a parent ion tolerance of 0.50 Da, and oxidation of methionine and acrylamide adduct of cysteine were specified as variable modifications.

Statistical analyses

Statistical analyses were performed using GraphPad Prism software 4.0 (GraphPad Software, San Diego, CA, USA) using either one- or two-way ANOVA or the Student *t* test with $p<0.05$ taken as significant. Details of each test and any post-hoc tests performed are outlined in the figure legends.

Results

Inactivation of cellular enzymes on exposure to HOSCN

A dose-dependent loss in the activity of CK and GAPDH was observed on treatment of J774A.1 lysates (1×10^6 cells ml^{-1}) with HOSCN (5–20 μM; Figs. 1a and c). Similar behavior was observed on treatment of intact J774A.1 cells (1×10^6 cells ml^{-1}) with HOSCN (80–200 μM; Figs. 1b and d), though in this case, greater concentrations of HOSCN were required to observe enzyme inactivation. This is attributed to the reduced accessibility of the oxidant to the cytosolic enzymes, as HOSCN is not freely membrane permeable with this cell type [20].

The mechanism of HOSCN-induced enzyme inactivation was investigated further in experiments in which the isolated CK and GAPDH (5 μM) enzymes were treated with HOSCN (2.5–25 μM) for 5 and 30 min, respectively, before determination of enzyme activity. Exposure of CK to HOSCN again resulted in a dose-dependent loss in enzyme activity (Fig. 2a, black bars). With CK, enzyme inhibition was reversible after the addition of DTT (40 μM) with ≤5 μM HOSCN (Fig. 2a, white bars), consistent with the modification of the active-site thiol residue and formation of sulfenyl derivatives. More extensive oxidation was observed at higher concentrations of HOSCN (10–25 μM), shown by the inability of DTT to regenerate enzymatic activity (Fig. 2a, white bars). Exposure of isolated GAPDH to HOSCN also led to a significant decrease in enzyme activity (Fig. 2b, black bars). With GAPDH, HOSCN-mediated inhibition was reversible after the addition of DTT (40 μM), at all concentrations of HOSCN employed (Fig. 2b, white bars).

In each case, a significant (>80%) loss in protein thiol concentration was observed on treatment of the isolated enzymes with an equimolar concentration of HOSCN (4.4 ± 0.8 to 0.9 ± 0.4 pmol thiol μg^{-1} protein for CK and 5.3 ± 1.5 to 0.6 ± 0.4 pmol thiol μg^{-1} protein for GAPDH) as assessed by the ThioGlo-1 assay. In addition, evidence was obtained for the formation of protein-derived, TNB-reactive species on reaction of both CK (14.1 ± 2.9 pmol μg^{-1} protein) and GAPDH (8.8 ± 1.2 pmol μg^{-1} protein) with HOSCN. In these experiments, care was taken to remove any residual HOSCN by gel filtration (PD-10 column) before assay with TNB. The formation of protein-derived, TNB-reactive species accounts for 62 and 32% of the initial HOSCN added to CK and GAPDH, respectively.

Formation and stability of sulfenyl thiocyanate species on CK and GAPDH

The formation of TNB-reactive species on CK and GAPDH after exposure to HOSCN is consistent with the formation of reactive protein-derived sulfenyl species. CK and GAPDH (25 μM) were exposed to HOS^{14}CN (12.5–50 μM) before precipitation of the protein and quantification of the extent of ^{14}C incorporation by scintillation counting. Experiments were performed in the presence and absence of DTT (1.25 mM) as RS–SCN adducts are readily reduced. Treatment of CK with increasing concentrations of HOS^{14}CN resulted in a dose-dependent increase in ^{14}C incorporation (Fig. 3a, white bars). After the addition of DTT, a significant loss in protein-associated ^{14}C was observed (Fig. 3a, gray bars). At the highest HOS^{14}CN dose (50 μM, twofold molar excess), a significant proportion of the ^{14}C label remained associated with the protein, even in the presence of DTT, suggesting formation of stable ^{14}C-containing protein products (Fig. 3a, gray bars). Similar results were observed in

analogous experiments with GAPDH (Fig. 3b). For both CK and GAPDH, no significant incorporation of the ^{14}C label was observed on treating the proteins with oxidant-free $S^{14}CN$ solutions (Figs. 3a and b, black and striped bars).

To assess the stability of products formed, CK and GAPDH (25 μM) were exposed to radiolabeled $HOS^{14}CN$ (25 μM) for up to 48 h. Treatment of CK with $HOS^{14}CN$ over time led to a significant increase in both DTT-reversible (Fig. 4a, circles) and irreversible ^{14}C-containing products (Fig. 4a, triangles). Similar results were obtained in experiments with GAPDH (Fig. 4c). However, in this case a decrease in the level of DTT-reversible, ^{14}C-containing products was observed after 48 h incubation (Fig. 4c, triangles). This is consistent with the decomposition of RS–SCN products, as reported previously [32].With both proteins, a significant increase in nonreversible product formation was observed on incubation of CK and GAPDH with HOSCN for 48 h (Figs. 4a and c).

The potential role of SCN^- and HOSCN-derived decomposition products in the modification of CK and GAPDH on prolonged incubation was assessed in experiments in which the proteins were treated with $HOS^{14}CN$ as described above, before isolation of the protein by gel filtration through PD-10 columns. After this treatment, the concentration of DTT-reversible products remained similar over 48 h with CK (Fig. 4b). In contrast, a decrease in the concentration of ^{14}C-containing, DTT-reversible, products was seen on incubation of HOSCN-treated GAPDH for ≥24 h (Fig. 4d). In each case, a significant increase in the formation of nonreversible products containing ^{14}C was also observed. Again, only low levels of ^{14}C incorporation were observed in control experiments with oxidant-free, $S^{14}CN^-$ solutions, with no changes seen on incubation over 48 h in the presence or absence of DTT (data not shown).

Formation of sulfenic acids and related oxidation products on CK and GAPDH

The susceptibility of the CK and GAPDH thiol residues to oxidation on exposure of the proteins to HOSCN was established using a peptide mass-mapping approach. The formation of sulfenic acid intermediates was examined using the chemical probe dimedone, which displays selectivity for these reactive species [38,39].

Creatine kinase

CK (25 μM) was exposed to HOSCN (12.5–125 μM) for 5 min, before incubation with dimedone (2 h, 200-fold molar excess), reductive alkylation with iodoacetic acid, and overnight digestion with trypsin. The resulting tryptic peptides were identified by searching the ExPASy database using the UniProtKB search engine; an 88% coverage of the CK sequence was obtained (Supplementary Table 1). A dose-dependent decrease in the abundance of a peak with *m/z* 1465.6 (retention time, 25.5 min) was observed on addition of HOSCN (Figs. 5a and 6a). This mass corresponds to the doubly charged peptide containing the alkylated active-site Cys-282 residue (Cys-282 + 58; position 266–291, $[M + H]^+$, 2930.2). The identity of this peak was confirmed by MS/MS analyses of the doubly charged species ($[M + 2H]^{2+}$, 1465.6, Fig. 6a).

HOSCN treatment also resulted in the detection of a new peak (retention time, 28.0 min) with *m/z* 1505.6 (the doubly charged peptide corresponding to $[M + H]^+$, 3010.2) (Fig. 5b). These parameters correspond to a mass increase of + 138 compared to the native, nonalkylated, peptide containing the active-site Cys-282, consistent with the formation of a dimedone adduct. The abundance of the dimedone-containing peptide (Cys-282 + 138) was most prevalent at the lowest HOSCN to CK ratio (0.5:1) (Fig. 5b). Subsequent MS/MS analyses of the $[M + 2H]^{2+}$ ion (*m/z* 1505.6) gave a series of both *y* and *b* fragment ions that

confirmed Cys-282 as the position of dimedonyl modification (Figs. 6a and b), consistent with formation of a sulfenic acid intermediate at the active-site Cys-282 residue.

In addition to the formation of a dimedone adduct, evidence was obtained for the formation of two new peaks at 25.9 and 23.9 min with *m/z* 1452.6 and 1460.6, respectively. These masses are consistent with the doubly charged species of peptides with +32 ($[M + H]^+$, 2904.2) and +48 ($[M + H]^+$, 2920.2) modifications to the native, nonalkylated, Cys-282 peptide. The abundance of these peaks was significantly increased on treatment of CK with equimolar or greater excesses of HOSCN (Figs. 5c and d). MS/MS analyses of the $[M + 2H]^{2+}$ parent ions (*m/z* 1452.6, *m/z* 1460.6) support the +32 and +48 modifications arising from the addition of two or three oxygen atoms to the Cys-282 residue (Figs. 6c and d). No significant loss in the abundance of any other CK native peptides was observed on exposure of the protein to HOSCN (up to a fivefold molar excess), including the peptides containing Cys-73 (position 43–85, $[M + H]^+$, 4677.1 monitored via the triply charged species, $[M + 3H]^{3+}$, 1559.7, retention time 24.7 min, Supplementary Fig. 1a), Cys-145 (position 138–147, $[M + H]^+$, 1189.3), or Cys-253 (position 251–258, $[M + H]^+$, 1009.2). However, evidence was obtained for increased formation of a new peptide ion with *m/z* 4757.1, consistent with the triply charged Cys-73 peptide being modified by dimedone (+138) rather than reductively alkylated (+58) (Supplementary Fig. 1b). MS/MS analysis of the new $[M + 3H]^{3+}$ peptide (*m/z* 1586.4, retention time 25.8 min) confirms addition of dimedone to the Cys-73 residue, providing evidence for the formation of an additional sulfenic acid on CK exposed to HOSCN (Supplementary Figs. 2a and b). Unlike the active-site Cys-282, no evidence was obtained for the formation of peptides with mass increases of +32 or +48, suggesting that Cys-73 is not overoxidized under the conditions used in this study.

Glyceraldehyde-6-phosphate dehydrogenase

Untreated GAPDH was digested using trypsin as described for CK, resulting in a 45% coverage of the GAPDH sequence (Supplementary Table 2). On treatment of GAPDH (25 μM) with HOSCN (12.5–125 μM) for 30 min, a dose-dependent loss (Fig. 7a) of the native peptide (retention time, 18.1 min; Fig. 8a) containing the active-site Cys-149 residue was observed. For GAPDH, the peptide containing the active-site Cys also contains an additional Cys residue, Cys-153; in the native peptide both Cys residues are reductively alkylated (position 143–159, $[M + H]^+$, 1823.0). HOSCN treatment of GAPDH resulted in the enhanced formation of a series of peptides corresponding to a combination of one alkylated Cys residue and an increase of +138 ($[M + H]^+$, 1903.0; retention times 21.1 and 22.1 min), +32 ($[M + H]^+$, 1797.0; retention time 17.0 min), or +48 ($[M + H]^+$, 1813.0; retention time 15.9 min) to the second nonalkylated Cys residue (Figs. 7b–d). Further MS/MS analysis of the $[M + 2H]^{2+}$ ion (*m/z* 952.0) established that the +138 mass increase was associated with conversion of either Cys-149 or Cys-153 to a dimedone adduct (Figs. 8b and c). Assuming that the two dimedone-containing peptides exhibit the same ionization efficiency, addition of dimedone to the Cys-149 (active-site) position was most prevalent on treatment of GAPDH with a substoichiometric concentration of HOSCN (12.5 μM) (Fig. 7b, black bars), whereas modification at the Cys-153 residue was more apparent at the highest oxidant dose employed (125 μM) (Fig. 7b, white bars). No evidence was obtained for the formation of a new peptide with amass increase of +276 (compared to the nonalkylated native peptide), suggesting that dimedone adduction, and hence sulfenic acid formation, does not occur simultaneously at both Cys residues.

Treatment of GAPDH with HOSCN also resulted in the increased detection of peptides with *m/z* 1797.0 and *m/z* 1813.0 (Figs. 7c and d), consistent with an oxidized Cys-149/Cys-153 peptide containing one alkylated Cys residue, with the second Cys residue modified with two or three oxygen atoms, respectively (Figs. 8d and e). Treatment of GAPDH with HOSCN also resulted in the formation of a peptide with a mass increase of +138 ($[M + H]^+$,

1638.7, retention time 25.0 min) compared to the native, nonalkylated Cys-244-containing peptide, though no significant loss of the alkylated peptide was detected (position 232–245, $[M + H]^+$, 1558.7; retention time 21.5 min; Supplementary Figs. 3a and b). MS/MS of the $[M + H]^+$ ion (*m/z* 1638.7) provided evidence for the formation of a dimedone adduct, indicative of sulfenic acid production at the Cys-244 site (Supplementary Figs. 4a and b). It remains to be established whether Cys-281 is also susceptible to HOSCN-induced oxidation, as the peptide containing this residue could not be detected under the conditions employed in this study. Further experiments utilizing alternative enzymes (chymotrypsin and endoproteinase GluC) for digesting the GAPDH also proved unsuccessful for studying the Cys-281 residue.

Dimedone and reactivity with RS-SCN

Dimedone reacts with sulfenic acid species [38]; however, its reactivity toward RS–SCN species has not been assessed. GAPDH (25 μM) was treated with equimolar $HOS^{14}CN$ and incubated in the presence and absence of dimedone for 2 h. After incubation, the protein was precipitated and ^{14}C incorporation assessed. A small, but significant, difference in DTT-irreversible ^{14}C incorporation onto GAPDH was observed in the presence of dimedone (0.14 ± 0.01 vs 0.12 ± 0.01 pmol of ^{14}C incorporation per μg of protein), suggesting that dimedone may influence the yield of RS–SCN intermediates to a minor extent.

Formation of sulfenic acids in cells exposed to HOSCN

The formation of sulfenic acid intermediates on cellular proteins in an intact cell model was examined in experiments using the cell-permeable, sulfenic acid-specific probe DAz-2 [40,41]. J774A.1 cells (1×10^6 cells ml^{-1}) were pretreated with DAz-2 (5 mM, in 1% v/v DMSO) before exposure to HOSCN (50–100 μM) for 15 min. This treatment resulted in the detection of a significant increase in biotinylated proteins (formed after p-biotin treatment of the samples and visualization with streptavidin–HRP) compared to untreated, control cells (Fig. 9). The increase in biotinylation observed was dependent on the concentration of HOSCN (50–100 μM). In contrast, only a few bands were observed in the absence of DAz-2. This is consistent with the majority of biotinylation being dependent on the binding of DAz-2 to cellular proteins, indicative of protein sulfenic acid formation. Coomassie staining of PVDF membranes verified equal protein loading in each case.

Evidence for the formation of GAPDH-derived, sulfenic acid species in cells exposed to HOSCN was obtained in experiments in which the membranes were reprobed with an anti-GAPDH antibody (data not shown). Analogous experiments with anti-CK were not conclusive, because of the nonspecific nature of the antibody in this case. Excision of the bands from the gels and LC–MS/MS sequencing after trypsin digestion confirmed that the HOSCN-dependent biotinylated protein bands of 37 and 43 kDa contained GAPDH and CK, respectively (Supplementary Table 5).

Discussion

Thiocyanate is the preferred substrate for the majority of mammalian peroxidases, including MPO, resulting in the production of significant concentrations of HOSCN under inflammatory conditions, particularly in smokers [21]. The role of HOSCN is traditionally viewed as bacteriostatic; however, an increasing number of studies highlight its role in cellular damage, via selective targeting of protein thiols [20,25–27,42], although the mechanism and intermediates involved in oxidative thiol modification in cells exposed to HOSCN are lacking. In this study, we show that HOSCN-mediated inactivation of the thiol-dependent enzymes CK and GAPDH involves the formation of sulfenyl thiocyanate and

sulfenic acid adducts. Direct evidence was also obtained for the formation of sulfenic acids on a range of proteins, including CK and GAPDH, on exposure of intact cells to HOSCN.

Treatment of J774A.1 cells with HOSCN resulted in a dose-dependent inhibition of CK and GAPDH activity. HOSCN is known to target GAPDH in bacterial cells, resulting in glycolysis arrest and inhibition of cell growth [22,43]. In this case, inhibition of GAPDH can occur in a reversible manner, supporting the formation of "sulfenyl" intermediates [22]. Inactivation of GAPDH has also been reported on exposure of various mammalian cell types to HOSCN (e.g., [19,42]). With J774A.1 cells, CK was more sensitive to inactivation than GAPDH. This is attributed to a difference in the active-site thiol pK_a (5.4 [44] and 8.2 [45] for CK and GAPDH, respectively), as HOSCN reacts more readily with low-pK_a thiol sites, with an inverse relationship between reaction rate and thiol group pK_a observed [46,47].

Reaction of HOSCN with isolated GAPDH and CK results in reversible enzyme inactivation in experiments with substoichiometric or equimolar amounts of oxidant. The loss of protein thiol residues, together with the detection of protein-derived, TNB-reactive species and the reversible incorporation of ^{14}C on exposure of the proteins to HOS^{14}CN, supports the generation of RS–SCN species, as reported previously [32,48]. With CK and GAPDH, these RS–SCN derivatives were long-lived at pH 7.4, with no significant decomposition detected over 24 h. This is in contrast to RS–SCN adducts formed on BSA, GSH, and penicillamine, which are short-lived under physiological conditions [32,49,50].

The reversible incorporation of ^{14}C in experiments with HOS^{14}CN may also be attributed to the formation of amino thiocyanate (R–NH–SCN) products. However, these species have been reported to be highly unstable at physiological pH [51]. Moreover, the concentration of protein thiols was in excess of the amount of oxidant added in this study, thus the formation of amino thiocyanate intermediates would not be expected.

In the presence of a molar excess of HOS^{14}CN compared to protein, and with prolonged incubation times, evidence was also obtained for the nonreversible incorporation of ^{14}C. This nonreversible incorporation may reflect protein carbamylation, owing to the formation of O^{14}CN$^-$ on the decomposition of HOS^{14}CN. Carbamylation may occur on either Cys, to produce thiocarbamate products, or Lys, resulting in homocitrulline formation [52]. Alternatively, it is possible that HOSCN induces modification of other non-Cys residues, such as Tyr or Trp, resulting in the formation of stable ^{14}C-containing products [22,32,53]. This is supported by studies showing nonreversible incorporation of ^{14}C but not ^{35}S on exposure of BSA to the LPO/H_2O_2/S^{14}CN or ^{35}SCN system, respectively, particularly under conditions where the concentration of H_2O_2 was greater than the level of protein thiols. This incorporation was attributed to the modification of aromatic amino acid residues by $(SCN)_2$, though it is possible that the presence of LPO influenced the distribution of products formed [48].

The stability of sulfenyl thiocyanate species is likely to be greatly influenced by the nature and loci of a protein or amino acid. Low-molecular-mass species react readily with reduced thiol groups to form disulfide bonds [50], whereas this reaction is disfavored with protein-derived species because of steric constraints [28,32]. It is postulated that hydrolysis of protein-derived sulfenyl thiocyanate species results in sulfenic acid formation (e.g., [28]), though direct experimental evidence for these species on exposure of proteins to HOSCN at physiological pH has been lacking. In this study, evidence for the formation of HOSCN-mediated protein-bound sulfenic acid intermediates on CK and GAPDH was obtained by the use of the sulfenic acid-specific trap dimedone and LC–MS peptide mass mapping. Sulfenic acid formation was observed at the active-site thiol groups of both CK and GAPDH, as evidenced by the detection of a peptide with a mass increase of +138, consistent with

dimedone addition. Dimedone reacts specifically with sulfenic acids and does not seem to react readily with sulfenyl thiocyanate species, as shown by only a minor loss in the extent of reversible ^{14}C incorporation in proteins exposed to HOS^{14}CN in the presence and absence of dimedone.

The greatest yield of active-site sulfenic acid species was observed on addition of substoichiometric levels of HOSCN, owing to overoxidation and the formation of sulfinic ($-SO_2H$) and sulfonic ($-SO_3H$) acids at greater than twofold molar excess of oxidant. In each case, the active-site thiol was the most susceptible to HOSCN-induced sulfenic acid formation, with oxidation of other thiol residues on CK and GAPDH observed at higher oxidant concentrations. The MS/MS fragmentation patterns of Cys–SO_2H-containing peptides are characteristically dominated by fragments corresponding to cleavage of the peptide C-terminal to the Cys–SO_2H, in addition to an increased abundance of fragment ions originating from neutral losses of H_2O and H_2SO_2, from the precursor and b_n fragment ions [54,55]. For CK, the fragmentation spectra of the Cys-282 + 32 peptide is dominated by fragments corresponding to C-terminal Cys–SO_2H cleavage (b_{17}) and neutral losses (H_2O, H_2SO_2) from the $[M + 2H]^{2+}$ species. In addition, an abundant y_9 ion is observed because of the presence of both a $-SO_2H$ on the Cys residue and the neighboring Pro residue, which are known to facilitate preferential peptide backbone cleavage (at the N-terminal side) [56]. In contrast, further oxidation of Cys–SO_2H to Cys–SO_3H does not result in enhanced fragmentation at the C-terminal side of Cys–SO_3H [54,55]. Consequently, the MS/MS spectra obtained from the Cys-282 + 48 peptide (Fig. 6d) more closely resembles the MS/MS spectra of the alkylated peptide (Fig. 6a) but with additional fragments due to the neutral loss of H_2O from the cysteic acid residue [54,55].

Similar fragmentation spectra are observed for the products assigned to be the sulfinic and sulfonic acid derivatives on the Cys-149 active site of GAPDH. The MS/MS fragmentation spectra of the peptide with addition of two oxygen atoms is dominated by ions characteristic of neutral losses of H_2O and H_2SO_2 from the $[M + 2H]^{2+}$ parent ion indicative of conversion of a Cys residue to a sulfinic acid (Fig. 8d). Similarly, the fragmentation spectra of the peptide with addition of three oxygen atoms is characteristic of conversion of a Cys residue to $-SO_3H$ (Fig. 8e). These results demonstrate that the active-site Cys-149 residue is markedly more sensitive to HOSCN-induced oxidation than Cys-153.

There are limited data to support the formation of sulfinic and sulfonic acids in HOSCN reactions in the literature. Exposure of bacterial cells to HOSCN is known to result in the formation of sulfenyl reactive species, and although increased exposure of cells to oxidants leads to the enhanced consumption of HOSCN, an overall decrease in reactive species (oxidizing equivalents) was observed. The continual consumption of HOSCN and parallel loss in functionality observed was attributed to the oxidation of the reactive sulfenyl species to higher oxy acids [22].

The formation of HOSCN-mediated sulfenic acids in a cellular environment was established using the dimedone analogue, DAz-2, a cell-permeable molecule linked to an azide “handle,” a modification that facilitates linking to biotin and subsequent detection with HRP–streptavidin [41]. A marked increase in the extent of biotinylated proteins after HOSCN treatment of intact J774A.1 cells in the presence of DAz-2 is consistent with the formation of intracellular protein-derived sulfenic acid species. Sulfenic acid formation was observed on many different cellular proteins, including CK and GAPDH, as evidenced by LC–MS sequencing studies, supporting the results from the experiments with the isolated enzymes in each case. The detection of protein-derived sulfenic acids in cells exposed to HOSCN has important implications in terms of the ability of this oxidant to modulate cellular function, as these species are increasingly being recognized as playing vital roles in

a vast array of cellular processes, including signaling cascades and the activation of transcription factors [57]. Indeed, it has been postulated that HOSCN modulates tissue factor release and the expression of cellular adhesion molecules in endothelial cells via redox activation of NF-κB, though the mechanism involved in this process remains to be elucidated [26].

In summary, this study provides the first direct evidence for the formation of protein sulfenic acids on exposure of both isolated proteins and mammalian cells to HOSCN. The selectivity of HOSCN for thiols, particularly low-pK_a thiols, and the ability to react in a reversible manner may ultimately result in a greater extent of cellular damage, compared to other, more potent MPO-derived oxidants. This is significant considering the high prevalence of low-pK_a thiols at enzymatic catalytic sites, which play an essential role in the regulation of protein structure and function and the modulation of signaling processes [58]. In addition, the ability of HOSCN to induce reversible thiol modifications suggests that this oxidant may have the potential to act as a second messenger in redox signaling processes. These results have important implications for the development and exacerbation of inflammatory disease and smoking-related pathologies.

Supplementary Material

Refer to Web version on PubMed Central for supplementary material.

Acknowledgments

This work was supported by grants from the National Heart Foundation (Australia) (CR0853959, GO753038, 632801) and the Australian Research Council (CE0561607, DP0988311). T.J.B. is grateful to the University of Sydney for the provision of an Australian Postgraduate Award scholarship. The authors also thank Dr Melanie White, University of Sydney, for her assistance with the LC–MS/MS protein sequencing studies.

Abbreviations

CK	creatine kinase
DAz-2	4-(3-azidopropyl)cyclohexane-1,3-dione
dimedone	5,5-dimethylcyclohexane-1,3-dione
DTT	dithiothreitol
GAPDH	glyceraldehyde-3-phosphate dehydrogenase
LC	liquid chromatography
MPO	myeloperoxidase
MS/MS	tandem mass spectrometry
RS–OH	sulfenic acid
R–SO_2H	sulfinic acid
R–SO_3H	sulfonic acid
RS–SCN	sulfenyl thiocyanate
SCN^-	thiocyanate ion
TCA	trichloroacetic acid
TFA	trifluoroacetic acid
TNB	5-thio-2-nitrobenzoic acid

References

1. Klebanoff SJ. Myeloperoxidase: friend and foe. J. Leukoc. Biol. 2005; 77:598–625. [PubMed: 15689384]
2. Davies MJ, Hawkins CL, Pattison DI, Rees MD. Mammalian heme peroxidases: from molecular mechanisms to health implications. Antioxid. Redox Signal. 2008; 10:1199–1234. [PubMed: 18331199]
3. Pruitt KM, Manssonrahemtulla B, Baldone DC, Rahemtulla F. Steady-state kinetics of thiocyanate oxidation catalyzed by human salivary peroxidase. Biochemistry. 1988; 27:240–245. [PubMed: 3349029]
4. Reiter B, Harnulv G. Lactoperoxidase antibacterial system—natural occurrence, biological functions and practical applications. J. Food Prot. 1984; 47:724–732.
5. Slungaard A, Mahoney JR Jr. Thiocyanate is the major substrate for eosinophil peroxidase in physiologic fluids: implications for cytotoxicity. J. Biol. Chem. 1991; 266:4903–4910. [PubMed: 2002037]
6. vanDalen CJ, Kettle AJ. Substrates and products of eosinophil peroxidase. Biochem. J. 2001; 358:233–239. [PubMed: 11485572]
7. van Dalen CJ, Whitehouse MW, Winterbourn CC, Kettle AJ. Thiocyanate and chloride as competing substrates for myeloperoxidase. Biochem. J. 1997; 327:487–492. [PubMed: 9359420]
8. Husgafvel-Pursiainen K, Sorsa M, Engstrom K, Einisto P. Passive smoking at work: biochemical and biological measures of exposure to environmental tobacco smoke. Int. Arch. Occup. Environ. Health. 1987; 59:337–345. [PubMed: 3610333]
9. Hampton MB, Kettle AJ, Winterbourn CC. Inside the neutrophil phagosome: oxidants, myeloperoxidase, and bacterial killing. Blood. 1998; 92:3007–3017. [PubMed: 9787133]
10. Winterbourn CC. Biological reactivity and biomarkers of the neutrophil oxidant, hypochlorous acid. Toxicology. 2002; 181–182:223–227.
11. Wu WJ, Chen YH, d'Avignon A, Hazen SL. 3-Bromotyrosine and 3,5-dibromotyrosine are major products of protein oxidation by eosinophil peroxidase: potential markers for eosinophil-dependent tissue injury in vivo. Biochemistry. 1999; 38:3538–3548. [PubMed: 10090740]
12. Wang J, Slungaard A. Role of eosinophil peroxidase in host defence and disease pathology. Arch. Biochem. Biophys. 2006; 445:256–260. [PubMed: 16297853]
13. Hawkins CL. The role of hypothiocyanous acid (HOSCN) in biological systems. Free Radic. Res. 2009; 43:1147–1158. [PubMed: 19905977]
14. Scanlon CEO, Berger B, Malcom G, Wissler RW. Evidence for more extensive deposits of epitopes of oxidized low density lipoproteins in aortas of young people with elevated serum thiocyanate levels. Atherosclerosis. 1996; 121:23–33. [PubMed: 8678921]
15. Botti TP, Amin H, Hiltscher L, Wissler RW. A comparison of the quantitation of macrophage foam cell populations and the extent of apolipoprotein E deposition in developing atherosclerotic lesions in young people: high and low serum thiocyanate groups as an indication of smoking. Atherosclerosis. 1996; 124:191–202. [PubMed: 8830932]
16. Wang Z, Nicholls SJ, Rodriguez ER, Kummu O, Horkko S, Barnard J, Reynolds WF, Topol EJ, DiDonato JA, Hazen SL. Protein carbamylation links inflammation, smoking, uremia and atherogenesis. Nat. Med. 2007; 13:1176–1184. [PubMed: 17828273]
17. Gould NS, Gauthier S, Kariya CT, Min E, Huang J, Brian DJ. Hypertonic saline increases lung epithelial lining fluid glutathione and thiocyanate: two protective CFTR-dependent thiols against oxidative injury. Respir. Res. 2010; 11:119–128. [PubMed: 20799947]
18. Tenovuo J, Larjava H. The protective effect of peroxidase and thiocyanate against hydrogen peroxide toxicity assessed by the uptake of [^{3}H]-thymidine by human gingival fibroblasts cultured in vitro. Arch. Oral Biol. 1984; 29:445–451. [PubMed: 6589987]
19. Bozonet SM, Scott-Thomas AP, Nagy P, Vissers MC. Hypothiocyanous acid is a potent inhibitor of apoptosis and caspase 3 activation in endothelial cells. Free Radic. Biol. Med. 2010; 49:1054–1063. [PubMed: 20615463]

20. Lloyd MM, Van Reyk DM, Davies MJ, Hawkins CL. HOSCN is a more potent inducer of apoptosis and protein thiol depletion in murine macrophage cells than HOCl or HOBr. Biochem. J. 2008; 414:271–280. [PubMed: 18459943]
21. Morgan PE, Pattison DI, Talib J, Summers FA, Harmer JA, Celermajer DS, Hawkins CL, Davies MJ. High plasma thiocyanate levels in smokers are a key determinant of thiol oxidation induced by myeloperoxidase. Free Radic. Biol. Med. 2011; 51:1815–1822. [PubMed: 21884783]
22. Thomas EL, Aune TM. Lactoperoxidase, peroxide, thiocyanate antimicrobial system: correlation of sulfhydryl oxidation with antimicrobial action. Infect. Immun. 1978; 20:456–463. [PubMed: 352945]
23. Oram JD, Reiter B. The inhibition of streptococci by lacteroperoxidase, thiocyanate and hydrogen peroxide—the oxidation of thiocyanate and the nature of the inhibitory compound. Biochem. J. 1966; 100:382–388. [PubMed: 5338806]
24. Carlsson J, Iwami Y, Yamada T. Hydrogen peroxide excretion by oral streptococci and effect of lactoperoxidase–thiocyanate–hydrogen peroxide. Infect. Immun. 1983; 40:70–80. [PubMed: 6832837]
25. Lane AE, Tan JT, Hawkins CL, Heather AK, Davies MJ. The myeloperoxidase-derived oxidant HOSCN inhibits protein tyrosine phosphatases and modulates cell signalling via the mitogen-activated protein kinase (MAPK) pathway in macrophages. Biochem. J. 2010; 430:161–169. [PubMed: 20528774]
26. Wang JG, Mahmud SA, Thompson JA, Geng JG, Key NS, Slungaard A. The principal eosinophil peroxidase product, HOSCN, is a uniquely potent phagocyte oxidant inducer of endothelial cell tissue factor activity: a potential mechanism for thrombosis in eosinophilic inflammatory states. Blood. 2006; 107:558–565. [PubMed: 16166591]
27. Wang JG, Mahmud SA, Nguyen J, Slungaard A. Thiocyanate-dependent induction of endothelial cell adhesion molecule expression by phagocyte peroxidases: a novel HOSCN-specific oxidant mechanism to amplify inflammation. J. Immunol. 2006; 177:8714–8722. [PubMed: 17142773]
28. Aune TM, Thomas EL. Oxidation of protein sulfhydryls by products of peroxidase-catalyzed oxidation of thiocyanate ion. Biochemistry. 1978; 17:1005–1010. [PubMed: 204336]
29. Parker DJ, Allison WS. The mechanism of inactivation of glyceraldehyde 3-phosphate dehydrogenase by tetrathionate, o-iodosobenzoate, and iodine monochloride. J. Biol. Chem. 1969; 244:180–189. [PubMed: 5773281]
30. Furtmuller PG, Jantschko W, Regelsberger G, Jakopitsch C, Arnhold J, Obinger C. Reaction of lactoperoxidase compound I with halides and thiocyanate. Biochemistry. 2002; 41:11895–11900. [PubMed: 12269834]
31. Nelson DP, Kiesow LA. Enthalpy of decomposition of hydrogen peroxide by catalase at 25°C (with molar extinction coefficient of H_2O_2 solution in the UV). Anal. Biochem. 1972; 49:474–478. [PubMed: 5082943]
32. Hawkins CL, Pattison DI, Stanley NR, Davies MJ. Tryptophan residues are targets in hypothiocyanous acid-mediated protein oxidation. Biochem. J. 2008; 416:441–452. [PubMed: 18652572]
33. Hawkins CL, Morgan PE, Davies MJ. Quantification of protein modification by oxidants. Free Radic. Biol. Med. 2009; 46:965–988. [PubMed: 19439229]
34. Eyer P, Worek F, Kiderlen D, Sinko G, Stuglin A, Simeon-Rudolf V, Reiner E. Molar absorption coefficients for the reduced Ellman reagent: reassessment. Anal. Biochem. 2003; 312:224–227. [PubMed: 12531209]
35. Allison WS, Kaplan NO. The comparative enzymology of triosephosphate dehydrogenase. J. Biol. Chem. 1964; 239:2140–2152. [PubMed: 14209940]
36. Cordwell SJ, Virginia L, Clark PMB. Acquisition and archiving of information for bacterial proteomics: from sample preparation to database. Methods Enzymol. 2002; 358:207–227. [PubMed: 12474389]
37. White MY, Cordwell SJ, McCarron HCK, Prasan AS, Craft G, Hambly BD, Jeremy RW. Proteomics of ischemia/reperfusion injury in rabbitmyocardium reveals alterations to proteins of essential functional systems. Proteomics. 2005; 5:1395–1410. [PubMed: 15800873]

38. Allison WS. Formation and reactions of sulfenic acids in proteins. Acc. Chem. Res. 1976; 9:293–299.
39. Seo YH, Carroll KS. Profiling protein thiol oxidation in tumor cells using sulfenic acid-specific antibodies. Proc. Natl. Acad. Sci. U. S. A. 2009; 106:16163–16168. [PubMed: 19805274]
40. Reddie KG, Seo YH, Muse WB, Leonard SE, Carroll K. A chemical approach for detecting sulfenic acid-modified proteins in living cells. Mol. Biosyst. 2008; 4:521–531. [PubMed: 18493649]
41. Leonard SE, Reddie KG, Carroll KS. Mining the thiol proteome for sulfenic acid modifications reveals new targets for oxidation in cells. Chem. Biol. 2009; 4:783–799.
42. Arlandson M, Decker T, Roongta VA, Bonilla L, Mayo KH, MacPherson JC, Hazen SL, Slungaard A. Eosinophil peroxidase oxidation of thiocyanate—characterization of major reaction products and a potential sulfhydryl-targeted cytotoxicity system. J. Biol. Chem. 2001; 276:215–224. [PubMed: 11013238]
43. Pruitt, KM.; Reiter, B. Biochemistry of peroxidase system: antimicrobial effects. In: Pruitt, KM.; Tenovuo, J., editors. The Lactoperoxidase System: Chemistry and Biological Significance. New York: Dekker; 1985. p. 143p. 178
44. Wang P-F, McLeish MJ, Kneen MM, Lee G, Kenyon GL. An unusually low pKa for cys282 in the active site of human muscle creatine kinase. Biochemistry. 2001; 40:11698–11705. [PubMed: 11570870]
45. Polgar L. Ion-pair formation as a source of enhanced reactivity of the essential thiol group of d-glyceraldehyde-3-phosphate dehydrogenase. Eur. J. Biochem. 1975; 51:63–71. [PubMed: 235434]
46. Nagy P, Jameson GNL, Winterbourn CC. Kinetics and mechanisms of the reaction of hypothiocyanous acid with 5-thio-2-nitrobenzoic acid and reduced glutathione. Chem. Res. Toxicol. 2009; 22:1833–1840. [PubMed: 19821602]
47. Skaff O, Pattison DI, Davies MJ. Hypothiocyanous acid reactivity with low-molecular-mass and protein thiols: absolute rate constants and assessment of biological relevance. Biochem. J. 2009; 422:111–117. [PubMed: 19492988]
48. Aune TM, Thomas EL, Morrison M. Lactoperoxidase-catalyzed incorporation of thiocyanate ion into a protein substrate. Biochemistry. 1977; 16:4611–4615. [PubMed: 911776]
49. Lemma K, Ashby MT. Reactive sulfur species: kinetics and mechanism of the equilibrium between cysteine sulfenyl thiocyanate and cysteine thiosulfinate ester in acidic aqueous solution. J. Org. Chem. 2008; 73:3017–3023. [PubMed: 18351774]
50. Ashby MT, Aneetha H. Reactive sulfur species: aqueous chemistry of sulfenyl thiocyanates. J. Am. Chem. Soc. 2004; 126:10216–10217. [PubMed: 15315413]
51. Thomas EL. Lactoperoxidase-catalyzed oxidation of thiocyanate: equilibria between oxidized forms of thiocyanate. Biochemistry. 1981; 20:3273–3280. [PubMed: 7248282]
52. Stark GR. Modification of proteins with cyanate. Methods Enzymol. 1998; 25:579–584. [PubMed: 23014442]
53. Aune TM, Thomas EL. Accumulation of hypothiocyanite ion during peroxidase-catalyzed oxidation of thiocyanate ion. Eur. J. Biochem. 1977; 80:209–214. [PubMed: 562752]
54. Wang Y, Vivekananda S, Men L, Zhang Q. Fragmentation of protonated ions of peptides containing cysteine, cysteine sulfinic acid, and cysteine sulfonic acid. J. Am. Soc. Mass Spectrom. 2004; 15:697–702. [PubMed: 15121199]
55. Men L, Wang Y. Further studies on the fragmentation of protonated ions of peptides containing aspartic acid, glutamic acid, cysteine sulfinic acid, and cysteine sulfonic acid. Rapid Commun. Mass Spectrom. 2005; 19:23–30. [PubMed: 15570570]
56. Hunt DF, Yates JR, Shabanowitz J, Winston S, Hauer C. Protein sequencing by tandem mass spectrometry. Proc. Natl. Acad. Sci U. S. A. 1986; 83:6233–6237. [PubMed: 3462691]
57. Poole LB, Nelson KJ. Discovering mechanisms of signaling-mediated cysteine oxidation. Curr. Opin. Chem. Biol. 2008; 12:18–24. [PubMed: 18282483]
58. Paulsen CE, Carroll KS. Orchestrating redox signaling networks through regulatory cysteine switches. Chem. Biol. 2010; 5:47–62.

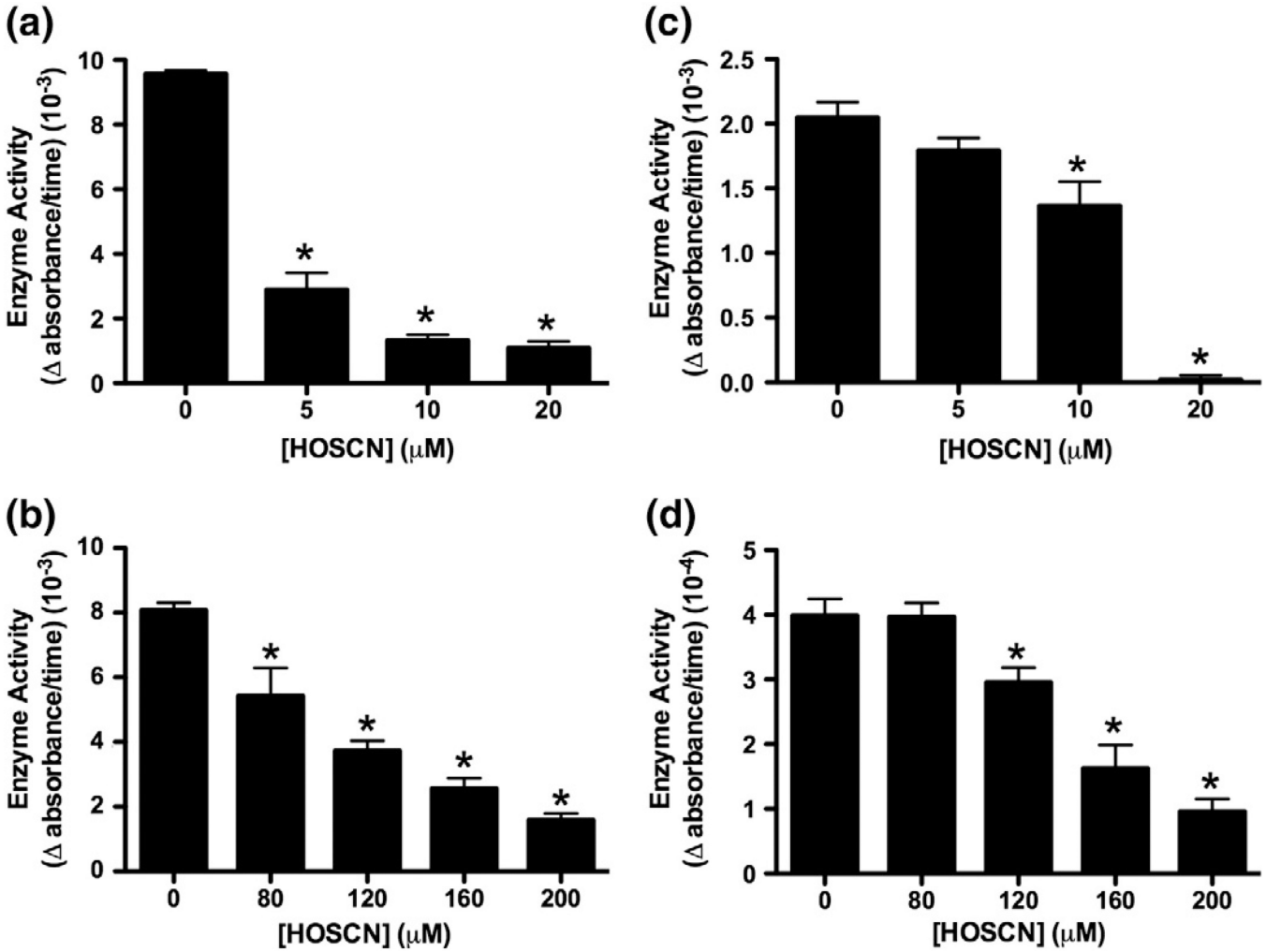

Fig. 1.

Inhibition of CK and GAPDH activity in J774A.1 lysates and intact cells after treatment with HOSCN. (a) CK and (c) GAPDH activity in J774A.1 cell lysates (1×10^6 cells ml^{-1}) after HOSCN treatment (5–20 μM) for 15 min at 22 °C. (b) CK and (d) GAPDH activity in intact J774A.1 cells (1×10^6 cells ml^{-1}) after HOSCN treatment (80–200 μM) for 15 min at 22 °C. *Significant decrease ($p<0.05$) in enzyme activity compared to control (untreated) lysates/cells by one-way ANOVA with Dunnett's post hoc test. Values are means ± SEM ($n = 6$).

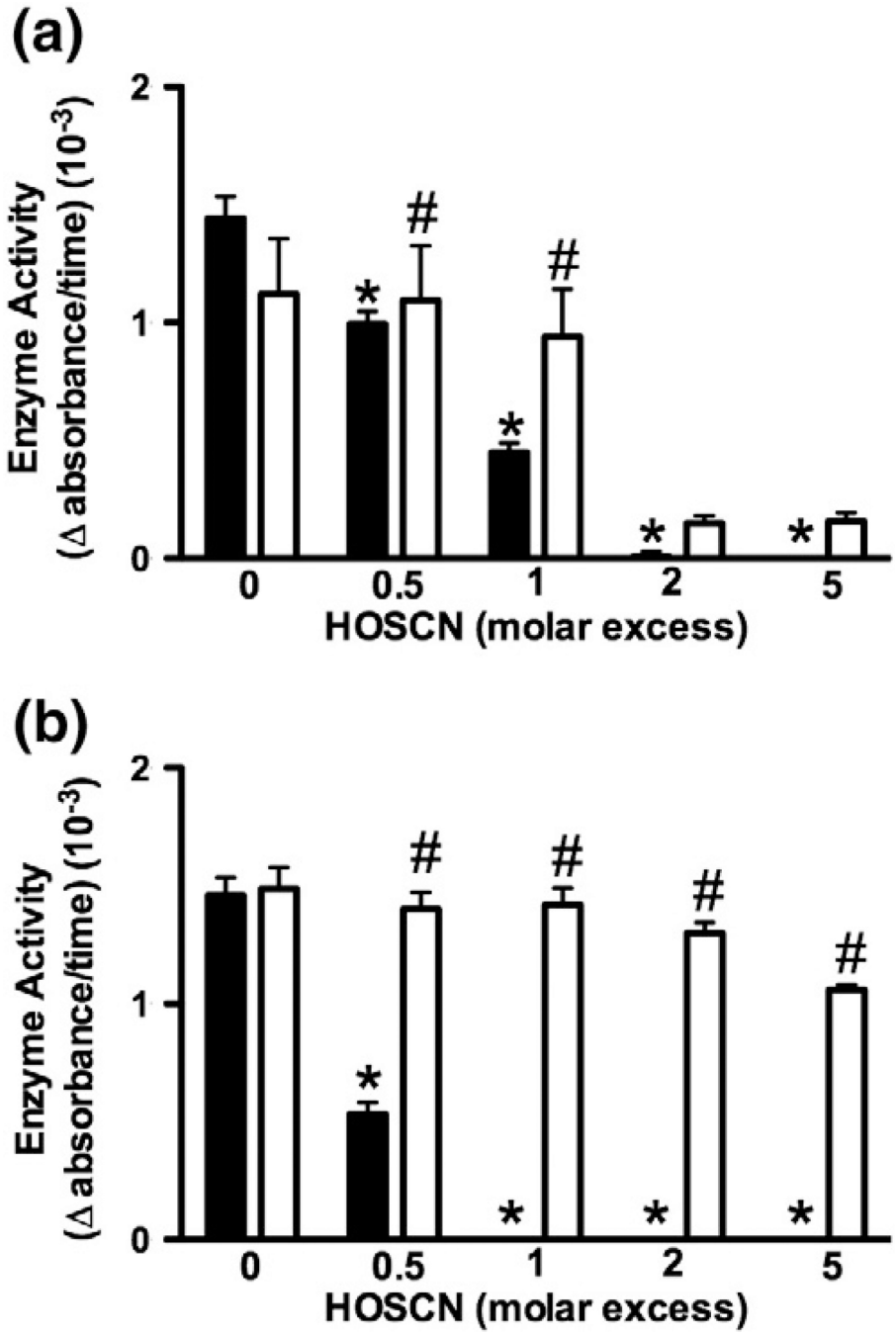

Fig. 2.

Inhibition of CK and GAPDH activity by HOSCN is reversible with DTT. (a) CK (5 μM) and (b) GAPDH (5 μM) were treated with HOSCN (2.5–25 μM) for 5 or 30 min, respectively, followed by further incubation in the absence (black bars) or presence (white bars) of DTT (40 μM) for 15 min. *Significant decrease (p<0.05) in enzyme activity of treated samples compared with controls by one-way ANOVA with Dunnett's post hoc testing; #significant increase (p<0.05) in enzyme activity on incubation in the presence of DTT compared to samples incubated in the absence of DTT by two-way ANOVA with Bonferroni post hoc testing. Values are means ± SEM (n = 6).

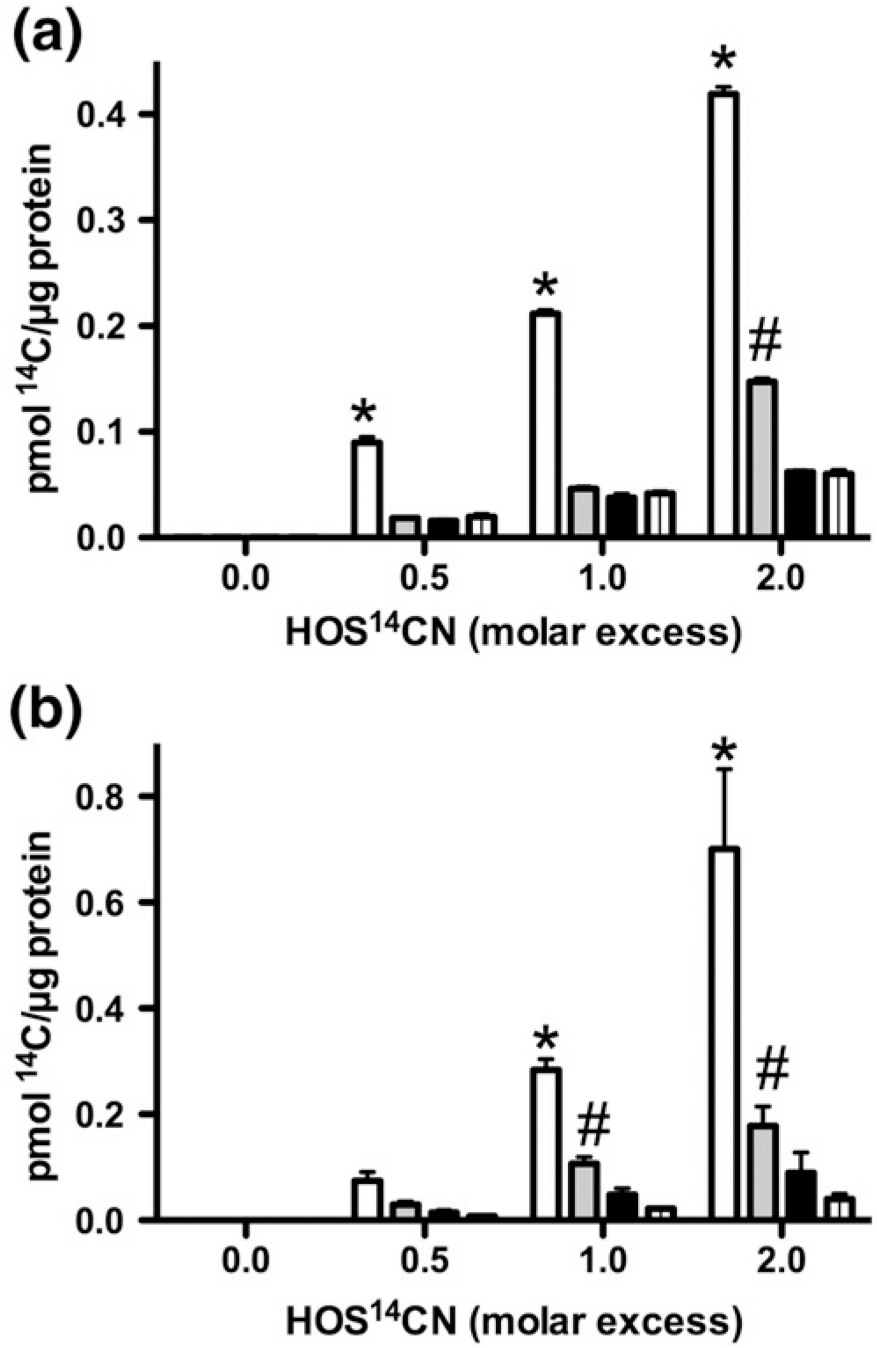

Fig. 3.

^{14}C incorporation after treatment of CK and GAPDH with HOS^{14}CN. (a) CK (25 µM) and (b) GAPDH (25 µM) were treated with HOS^{14}CN (12.5–50 µM) for 5 and 30 min, respectively, before incubation in the absence (white bars) and presence (gray bars) of DTT (1.25 mM). Controls were performed with oxidant-free, S^{14}CN$^-$ solutions with no DTT added (black bars) and after addition of DTT (1.25 mM; striped bars). A significant increase (p<0.05) in ^{14}C incorporation was seen, compared with the control treated with oxidant-free S^{14}CN$^-$ solutions in the (*) absence and (#) presence of DTT, using two-way ANOVA with Bonferroni post hoc testing. Values are means ± SEM (n≥5).

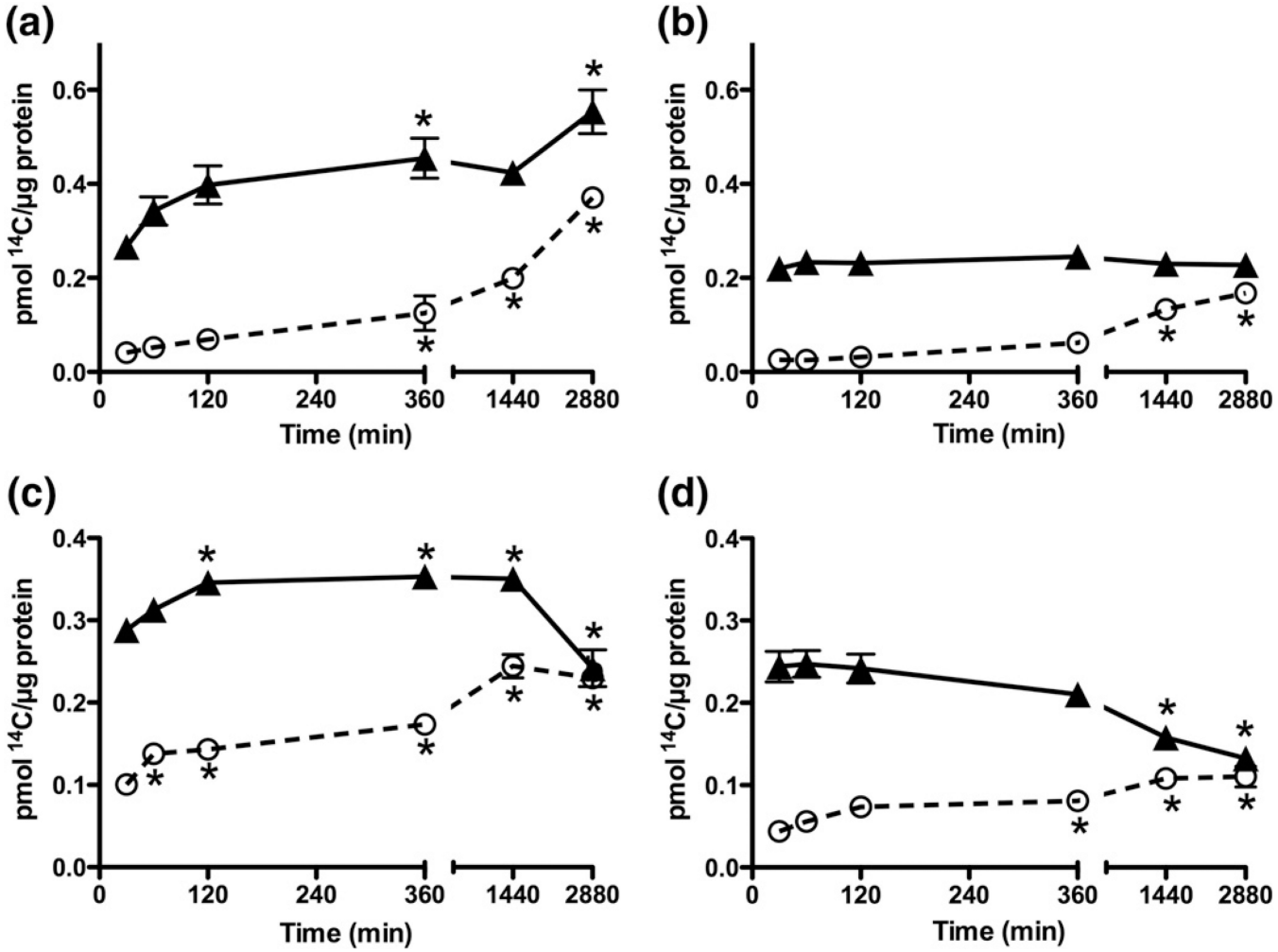

Fig. 4.

Effect of incubation time on the extent of ^{14}C incorporation after treatment of CK and GAPDH with HOS^{14}CN. (a) CK (25 µM) was treated with HOS^{14}CN (25 µM) for various times before further incubation in the absence (triangle) and presence of DTT (1.25 mM; circle). (b) CK (25 µM) was treated with HOS^{14}CN (25 µM) for 5 min before gel filtration to remove excess S^{14}CN^{-} and potential decomposition products and further incubation in the absence (triangle) and presence of DTT (1.25 mM; circle). (c) GAPDH (25 µM) was treated with HOS^{14}CN (25 µM) for various times before further incubation in the absence (triangle) and presence of DTT (1.25 mM; circle). (d) GAPDH (25 µM) was treated with HOS^{14}CN (25 µM) for 30 min before gel filtration and analysis as in (b). *p<0.05; significant increase or decrease in ^{14}C incorporation compared with initial incorporation by one-way ANOVA with Bonferroni post hoc testing. Values are means ± SEM (n≥5). Error bars have been plotted, but in some cases are smaller than the symbol used.

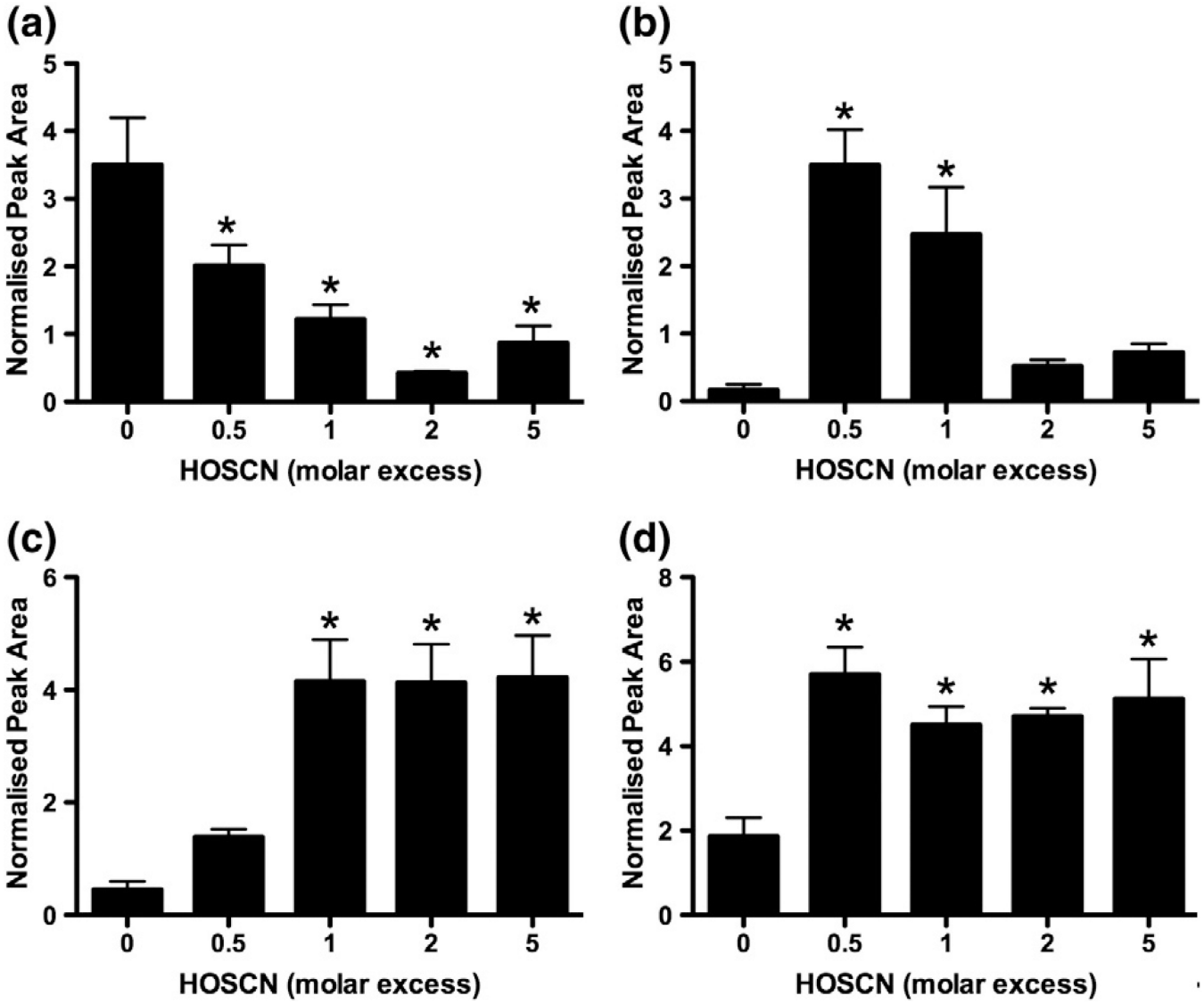

Fig. 5.

Treatment of CK with HOSCN results in oxidation of the active-site Cys-282. CK (25 μM) was treated with HOSCN (12.5–250 μM) for 5 min, before reductive alkylation, tryptic digestion, and LC–MS/MS analysis. (a) Loss of the alkylated active-site Cys-containing peptide of CK (Cys-282, $[M + 2H]^{2+}$, 1465.6). (b) Formation of the +138 product peptide corresponding to the addition of dimedone at the Cys-282 active-site of CK ($[M + 2H]^{2+}$, 1505.6). (c) Formation of the +32 product peptide corresponding to sulfinic acid generation at Cys-282 ($[M + 2H]^{2+}$, 1452.6). (d) Formation of the +48 product peptide corresponding to sulfonic acid generation at Cys-282 ($[M + 2H]^{2+}$, 1460.6). Peak areas were obtained from extracted ion chromatograms (selected characteristic ions presented in Supplementary Table 3) and were standardized to the area of the CK oxidant-insensitive peptide SEEEYPDLSK ($[M + 2H]^{2+}$, 598.5). *p<0.05; significant decrease or increase in the concentration of each peptide compared to control by one-way ANOVA with Dunnett's post hoc test. Values are means ± SEM (n = 6).

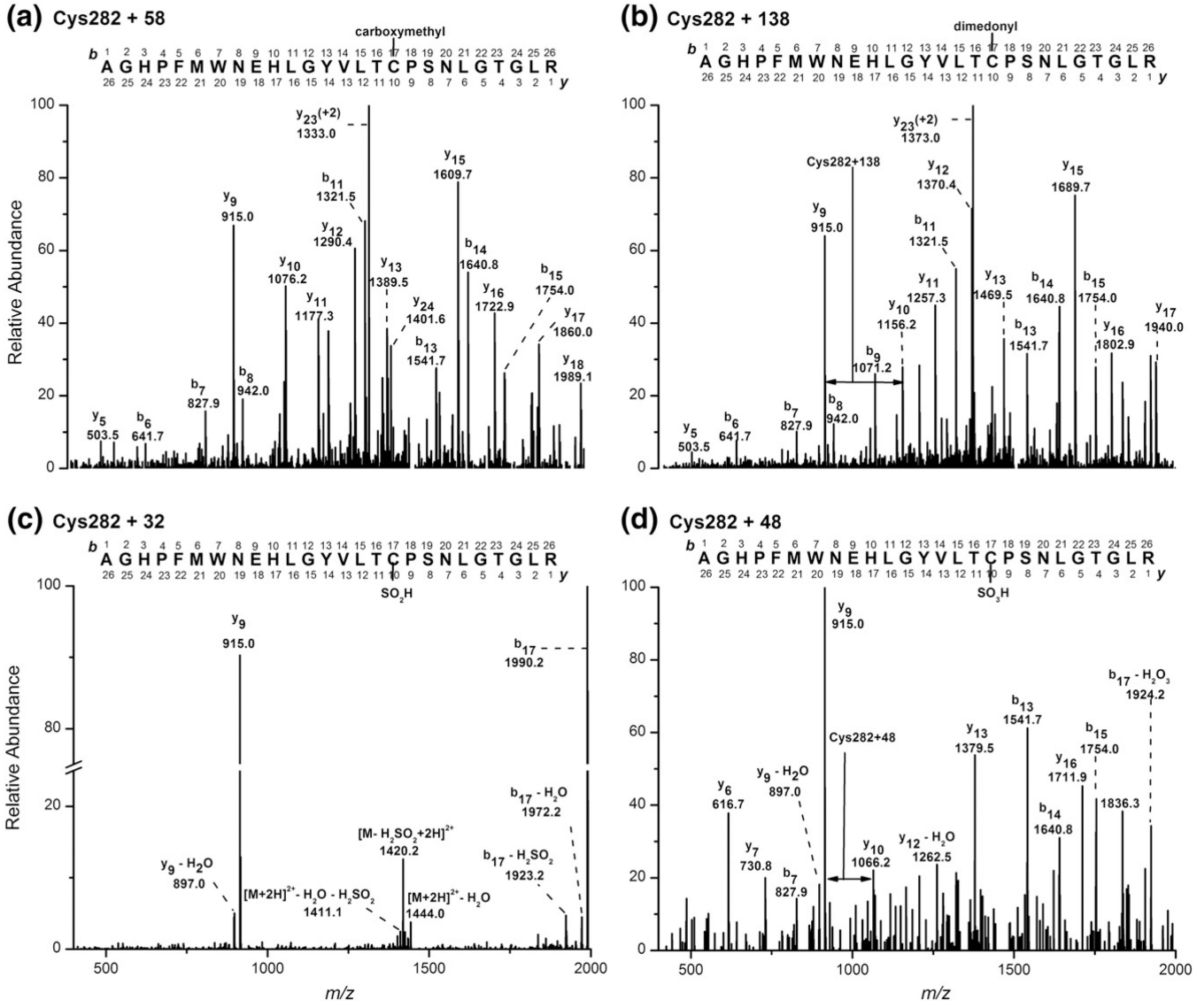

Fig. 6.

Fragmentation ion spectra of the $[M + 2H]^{2+}$, $[M + 138 + 2H]^{2+}$, $[M + 32 + 2H]^{2+}$, and $[M + 48 + 2H]^{2+}$ for the modified active-site (Cys-282) peptides from tryptic digests of HOSCN-treated CK. (a) MS/MS spectrum of the doubly charged species *m/z* 1465.6 (carboxymethyl peptide), with the fragment ions specific for the Cys-282 + 58 product. Fragment ions are singly charged, except where specified. Equivalent data are shown in (b), (c), and (d), obtained by monitoring the doubly charged peptide species *m/z* 1505.6, 1452.6, and 1460.6, respectively. Data are representative of at least five independent experiments.

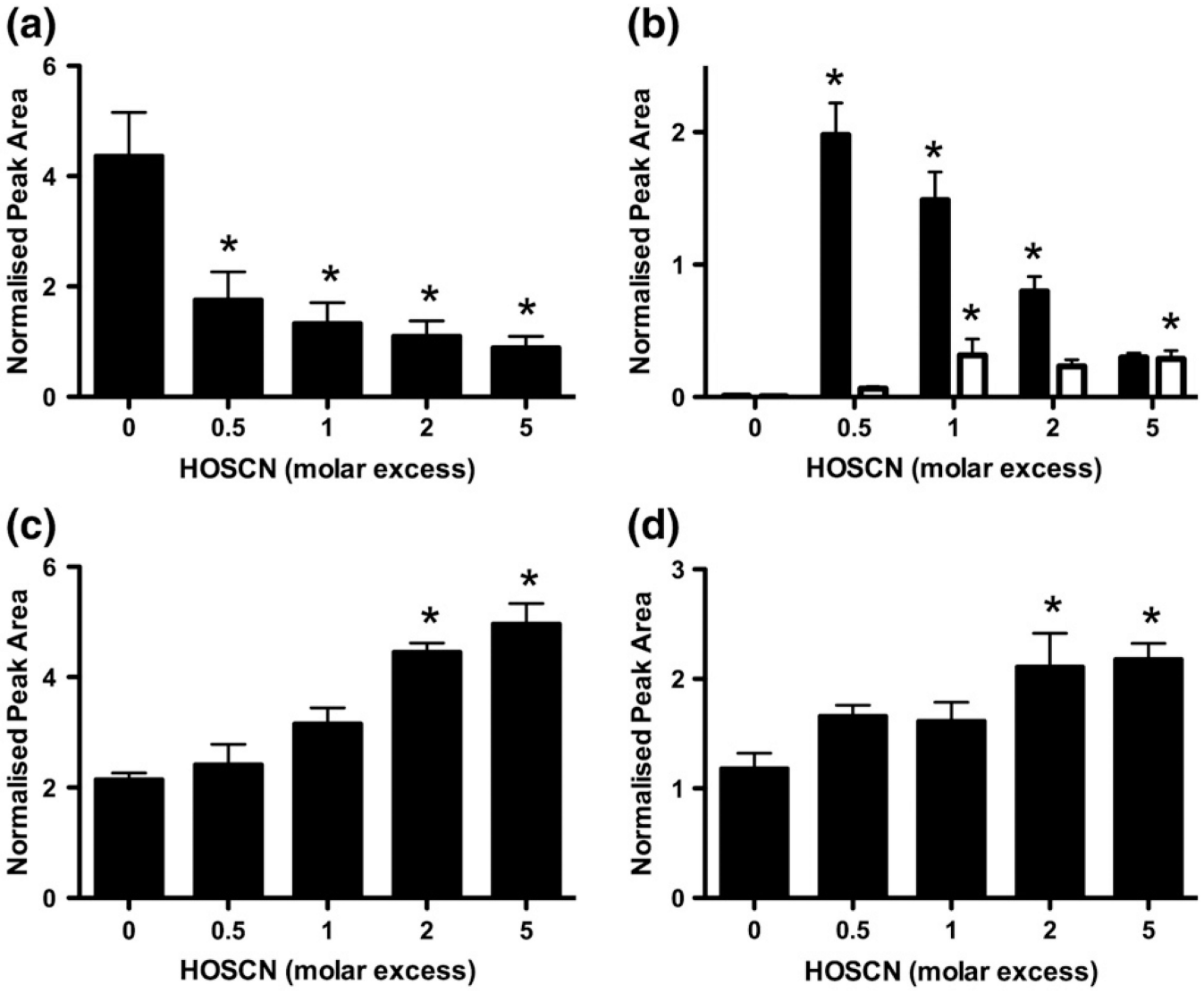

Fig. 7.

Treatment of GAPDH with HOSCN results in oxidation of Cys-149 and Cys-153. GAPDH (25 μM) was treated with HOSCN (12.5–250 μM) for 30 min, before reductive alkylation, tryptic digestion, and LC–MS/MS analysis. (a) Loss of the active-site Cys-containing peptide of GAPDH (Cys-149, $[M + 2H]^{2+}$, 912.0). (b) Formation of the +138 product peptide corresponding to the addition of dimedone at the Cys-149 active site of GAPDH (black bars, $[M + 2H]^{2+}$, 952.0) and addition of dimedone at the Cys-153 site of GAPDH (white bars, $[M + 2H]^{2+}$, 952.0). (c) Formation of the +32 product peptide corresponding to sulfinic acid generation on Cys-149 ($[M + 2H]^{2+}$, 899.0). (d) Formation of the +48 product peptide corresponding to sulfonic acid generation on Cys-149 ($[M + 2H]^{2+}$, 907.0). Peak areas were obtained from extracted ion chromatograms (selected characteristic ions presented in Supplementary Table 4) and were standardized to the area of the oxidant-insensitive GAPDH peptide GAAQNIIPASTGAAK ($[M + 2H]^{2+}$, 685.6). *p<0.05; significant decrease or increase in the tryptic peptide of interest compared to control conditions by one-way ANOVA with Dunnett's post hoc test. Values are means ± SEM (n = 6).

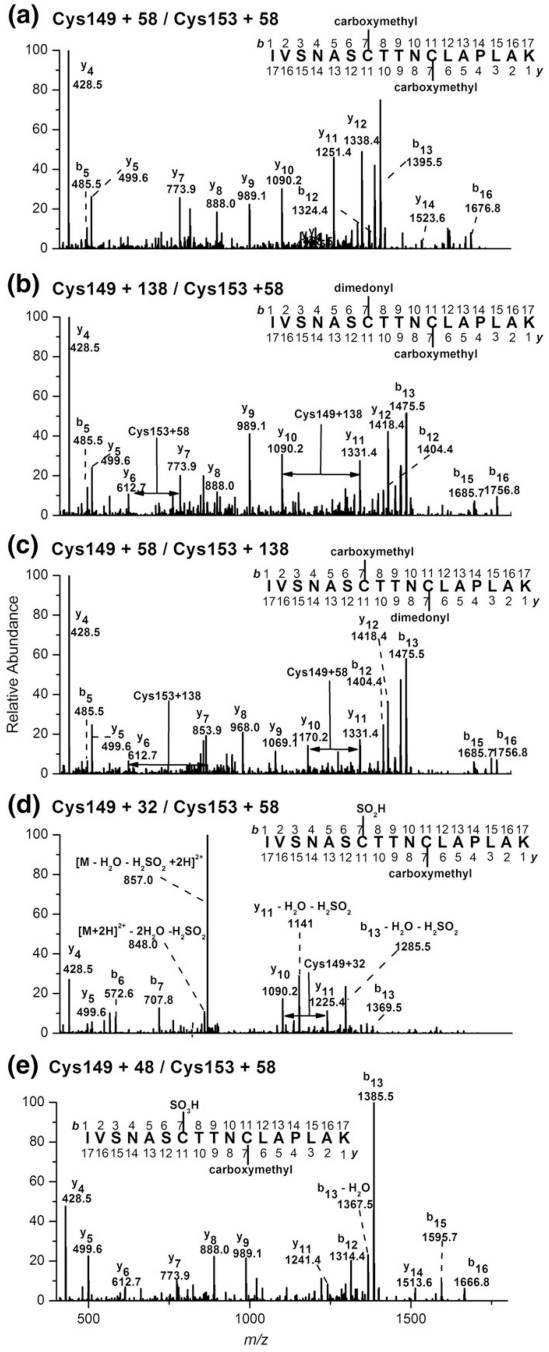

Fig. 8.

Fragmentation ion spectra of $[M + 2H]^{2+}$, $[M + 138 + 2H]^{2+}$ (Cys-149 and Cys-153), $[M + 32 + 2H]^{2+}$ (Cys-149), and $[M + 48 + 2H]^{2+}$ (Cys-149) peptides from tryptic digests of HOSCN-treated GAPDH. (a) MS/MS spectrum of the doubly charged species *m/z* 912.0 (carboxymethyl peptide), with the fragment ions specific for the Cys-149 + 58 and Cys-153 + 58 product. Fragment ions are singly charged. Equivalent data are shown in (b), (c), (d), and (e) via monitoring of the doubly charged species *m/z* 952.0, 899.0, and 907.0, respectively. Data are representative of at least five independent experiments.

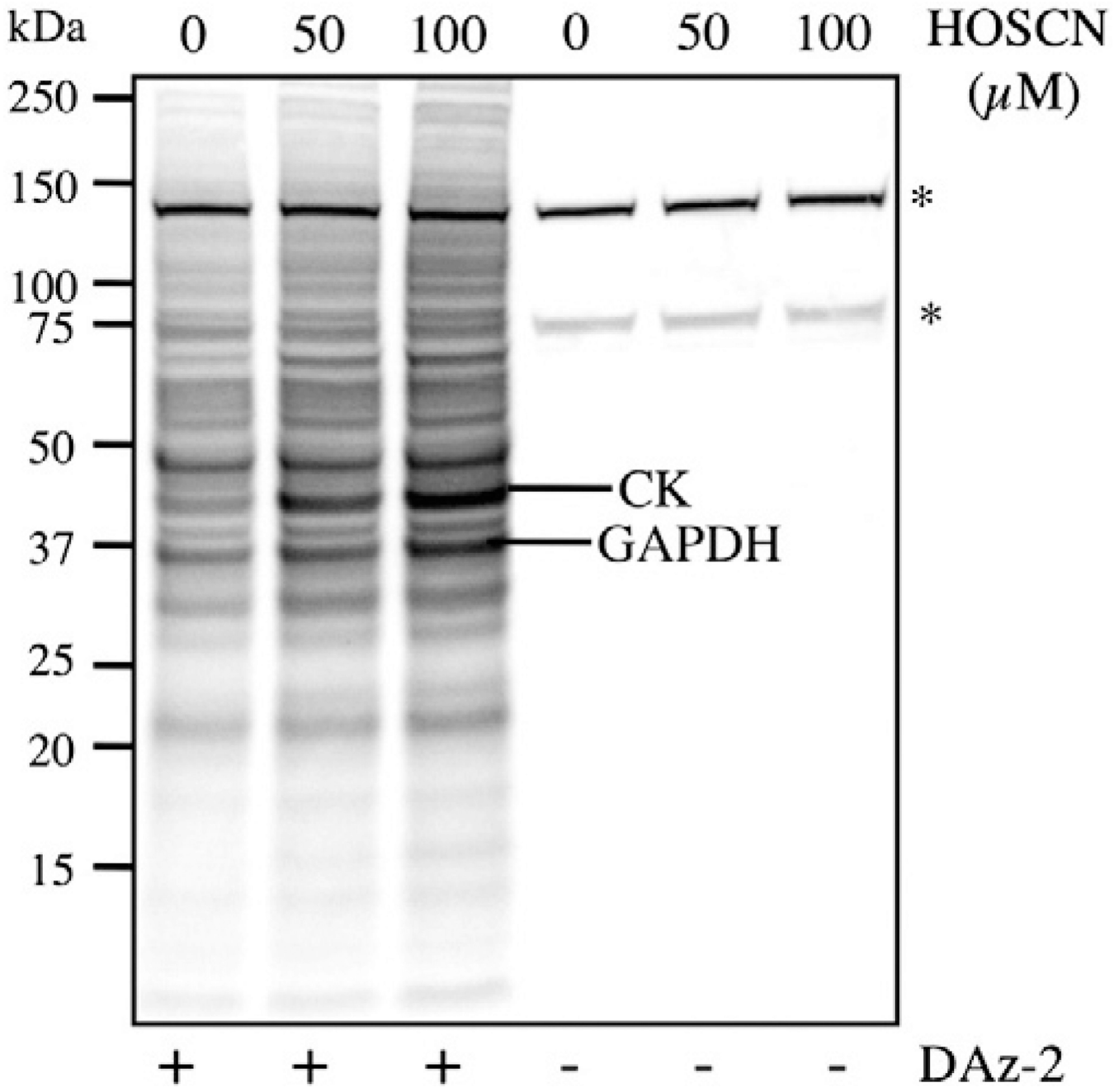

Fig. 9.

Exposure of J774A.1 cells to HOSCN results in the formation of protein-derived sulfenic acid species. J774A.1 cells (1×10^6 cells ml^{-1}) were pretreated with DAz-2 (5 mM in 1% v/v DMSO) or DMSO (1% v/v) for 30 min at 37 °C before the addition of PBS or HOSCN (50–100 μM) and further incubation for 15 min at 37 °C. The cells were then lysed, and Staudinger ligation was carried out with p-biotin (200 μM) and DTT (5 mM) for 2 h at 37 °C. The reaction was quenched and proteins were separated by 1D SDS–PAGE (4–12%). Proteins (50 μg per lane) were then transferred to PVDF membranes and biotinylated proteins detected by HRP–streptavidin. Asterisks denote endogenously biotinylated proteins.